River Flow 2012 – Murillo (Ed.)
© 2012 Taylor & Francis Group, London, ISBN 978-0-415-62129-8

Quasi-3D modelling of bed shear stresses at high curvature

W. Ottevanger & W.S.J. Uijttewaal
Faculty of Civil Engineering and Geosciences, Delft University of Technology, The Netherlands

K. Blanckaert
State Key Laboratory of Urban and Regional Ecology, Research Center for Eco-Environmental Sciences, Chinese Academy of Sciences, Beijing, China
Laboratory of Hydraulic Constructions (LCH), Ecole Polytechnique Fédérale de Lausanne (EPFL), Lausanne, Switzerland
Faculty of Civil Engineering and Geosciences, Delft University of Technology, The Netherlands

ABSTRACT: Single thread meandering rivers exhibit complex planform patterns in their floodplains, resulting from a complex interaction between flow, bed and bank morphology. The flow through meander bends may be characterized by primary flow in streamwise direction and secondary flow in transverse direction. The secondary flow plays an important role in the redistribution of streamwise momentum and also affects the bed shear stress, which is important for the shaping of the bed topography.

Presently, most depth-averaged morphodynamic models adopt a secondary flow parameterization, based on mild curvature assumptions. This yields a linear relation between curvature and secondary flow strength. However, in strongly curved river bends, the secondary flow strength weakens considerably, due to the non-linear interaction of the streamwise and transverse velocity profiles. This interaction does not only affect the redistribution of streamwise momentum, but it is also important for the direction and magnitude of the bed shear stresses.

A non-linear quasi-3D hydrodynamic model (i.e. depth averaged plus 3D parameterizations) is presented and used to simulate two sharply curved flume experiments over a horizontal and fully developed bed. The hydrodynamics results are compared to measurements, a three-dimensional hydrodynamic model, a three-dimensional hydrodynamic model with few layers, a linear hydrodynamic model based on mild curvature assumptions, and a depth-averaged model without secondary flow.

The non-linear quasi-3D model results show a qualitatively good agreement with measurements and the three dimensional model. The linear quasi-3D model overestimates the angle between the bed shear stress and the depth averaged velocity direction through the bend. Furthermore the linear model fails to capture the increase of bed shear stress magnitude correctly. The depth-averaged model without secondary flow shows no increase of bed shear stress magnitude and no angle between the bed shear stress and the depth averaged velocity direction. Over the horizontal bed the 3D model with a small number of vertical layers underestimates the bed shear stress angle as well as the increase of bed shear stress magnitude. Over the fully developed bed the 3D model with a small number of vertical layers shows an underestimation of the increase of bed shear stress, but shows good agreement for the bed shear stress angle.

1 INTRODUCTION

Meandering single thread rivers are known to wind their way through floodplains. Many scientists from various disciplines have studied meander behavior (see Camporeale et al., 2007, and the references therein). The recent attention for renaturalization projects has lead decision makers to consider the partial remeandering of previously trained rivers. Factors such as navigation and man-made infrastructure along the river set limits for the maximum migration of such rivers. Therefore, models that can predict the evolution of meandering rivers are required. Meander evolution is primarily driven by the flow; therefore the present paper will focus on the flow and its forcing on the river boundaries.

The complex hydrodynamics in river bends can be split into primary flow in streamwise direction and secondary flow normal to the primary flow (cf. Figure 1). Accurately modeling the flow in river bends requires the use of a three dimensional flow model. Even though computing power is rapidly increasing, three dimensional (3D) simulations of long river reaches including morphological development are still too demanding. Therefore, river engineers divert to the use of reduced models (e.g. depth and/or width averaged).

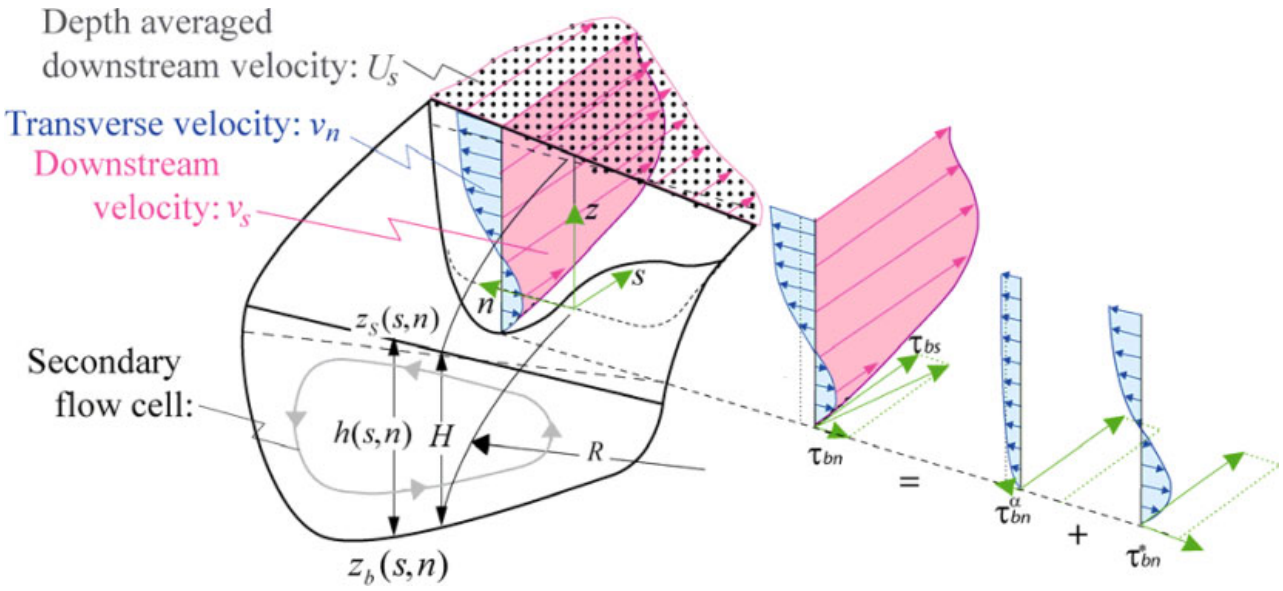

Figure 1. Definition sketch and velocity and bed shear stress decomposition (adapted from Blanckaert and de Vriend 2010).

Extending such reduced models with a parameterization for 3D effects yields so-called quasi-3D models.

Helical or secondary flow is an example of such an effect that requires parameterization. Secondary flow is important for redistributing streamwise momentum over the cross-section, as was shown by Johannesson and Parker (1989b), Blanckaert and de Vriend (2010) and Ottevanger et al. (2011). Secondary flow also influences the magnitude and direction of the bed shear stress, which are obviously very important when considering morphodynamic evolution.

At present, the parameterization of the bed shear stress in reduced morphodynamic models is only valid for mildly curved flow ($B/R << 1$) (see e.g. Rosovskii 1957, Engelund 1974, Kikkawa, 1976 and de Vriend 1977). Recently however, by including the non-linear interaction between streamwise and secondary flow, Blanckaert & de Vriend (2003) developed a non-linear parameterization of secondary flow and bed shear stress which is also valid for strongly curved flow.

There are two main differences between the linear and non-linear parameterization for the bed shear stress at high curvature. Firstly, compared to the linear parameterization, the non-linear one shows a reduction in the angle between the bed shear stress and the depth-averaged flow. Secondly, the non-linear parameterization shows an increase in the magnitude of the bed shear stress compared to the linear bed shear stress magnitude.

The motivation for the development of Q3D models is related to i) understanding of the dominant physical processes in the system, ii) having a simple model available when input data is scarce, and iii) Q3D models are faster than their 3D counterparts, while still giving a reasonable prediction of processes caused by the three dimensionality of the flow.

In this study, a quasi-3D hydrodynamics solver with i) non-linear parameterization, ii) linear parameterization and iii) without parameterization is applied to a strongly curved bend experiment. The results will be compared to the measured data and to a 3D simulation as well as a 3D simulation with a small number of vertical layers.

2 BED SHEAR STRESSES

Bed shear stresses play an important role in open channel flow. On the one hand they represent the friction of the flow on the boundaries, which deter-mines the conveyance capacity and the water levels. On the other hand they are important for determining the morphodynamic evolution of the bed.

The equation governing the morphodynamic evolution is known as the Exner balance, and in curvilinear coordinates, it is given by:

$$\left(1-\varepsilon_p\right)\frac{\partial z_b}{\partial t}+\frac{1}{1+n/R}\frac{\partial s_{bs}}{\partial s}+\frac{\partial s_{bn}}{\partial n}+\frac{1}{1+n/R}\frac{s_{bn}}{R} \qquad (1)$$

where z_b is the bed elevation and s_{bs} and s_{bn} are the sediment transport capacity in streamwise and transverse direction, respectively. Mosselman (2005) showed that the majority of sediment transport formulae have a form which is given by:

$$\frac{s_b}{\sqrt{g\Delta D^3}}=a\theta^{n-\gamma}\left(\mu\theta-\theta_{cr}\right)^{\gamma} \qquad (2)$$

where s_b denotes the sediment transport magnitude, the relative density of a submerged sediment grain in water is given by $\Delta=(\rho_s-\rho)/\rho$. The dimensionless shear stress and dimensionless critical shear stress are given by $\theta=\tau_b/(\rho g\Delta D)$ and θ_{cr} respectively. The gravitational constant is given by g, D is a characteristic diameter of the sediment, μ is the ripple factor, n and γ are exponents, and a is a calibration factor. Consequently, the total sediment budget is determined by the distribution and direction of the bed shear stresses.

The bed shear stress and its direction require a parameterization as they are influenced by the three dimensionality of the flow. The parameterization consists of three steps, firstly a local parametrization is determined based on 1DV profiles determined by local flow properties on the centreline. Secondly, a distribution function is applied which extends the parameterization results over the width of the channel. Finally, inertia is included by means of an adaptation equation.

2.1 *Parameterization models on the centreline*

The sediment transport capacity given in Eq. (2) is based on the bed shear stress magnitude. A parameterization is needed for the bed shear stress magnitude which reads

$$\tau_b = \psi C_f U^2 \tag{3}$$

C_f denotes the friction factor, and it can be related to a Nikuradse roughness height k_s (see e.g. Vardy 1990) and U is the magnitude of the depth-averaged velocity. A correction factor ψ is included to model the increase of energy losses due to hydrodynamic curvature effects: The presence of secondary flow flattens the streamwise velocity profile, subsequently increasing the bed shear stress (Blanckaert & de Vriend, 2003).

In the linear parametrization models $\psi = \psi_0 = 1$. For strongly curved flow the increase of bed shear stress $\psi = \psi_\infty = f(\beta C_f^{0.15})$ is given by the function given in Figure 2a), determined by Blanckaert and de Vriend (2003) where β is the bend parameter defined in Figure 2b). The bend parameter depends on the water depth H, the centerline radius of curvature R, the friction factor C_f and α_s. The value of α_s is related to the normalized transverse gradient of the streamwise velocity at the centerline (which forms the key feedback mechanism of the non-linear model):

$$\frac{\alpha_s}{R} = \frac{1}{U_s}\frac{\partial U_s}{\partial n}\bigg|_{n=0} \tag{4}$$

The values $\alpha_s = -1$ and $\alpha_s = 1$, correspond to potential and forced vortex distributions respectively (cf. Vardy 1990).

The direction of motion of a sediment particle is influenced by the bed shear stress and the pull of gravity on sloping boundaries. Olesen (1987) summarized this as follows:

$$\frac{s_{bn}}{s_{bs}} = \frac{\tau_{bn}}{\tau_{bs}} - G\frac{\partial z_b}{\partial n} = \left(\frac{U_n}{U_s} + \frac{\tau^*_{bn}}{\tau_{bs}}\right) - G\frac{\partial z_b}{\partial n} \tag{5}$$

The direction of the bed shear stress can be decomposed into components related to the depth-averaged velocities U_s and U_n and components related to secondary flow (see Figure 1), whereby the latter component is parameterized by:

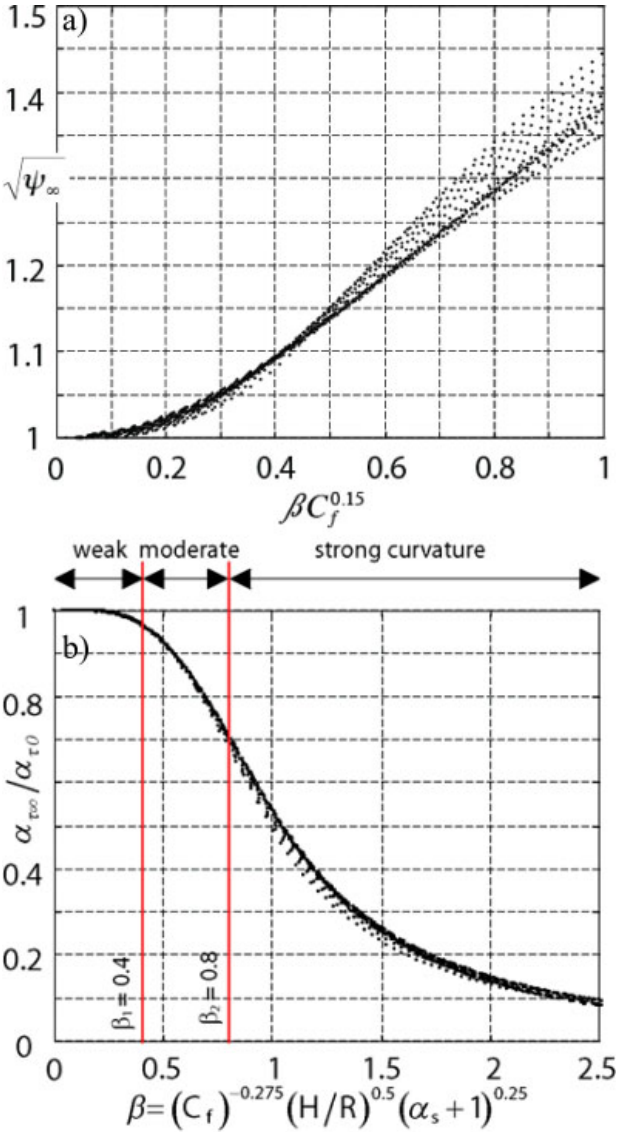

Figure 2. a) Increase of correction factor for the bed shear stress magnitude, ψ (top) and b) reduction factor $\alpha_{\tau\infty}/\alpha_{\tau 0}$ of the bed shear stress angle due secondary flow as function of the bend parameter β (bottom). Reprinted from Blanckaert and de Vriend (2003) with permission from the authors.

$$\frac{\tau^*_{bn}}{\tau_{bs}} = \alpha_\tau \frac{H}{R} f_w(n) \tag{6}$$

The function $f_w(n)$ is a distribution function which will be elaborated on in section 2.2. The parameterization term is α_τ which in the linear case ($\alpha_\tau = \alpha_{\tau 0}$) is given by the following equation (de Vriend 1977):

$$\alpha_{\tau 0} = 2\kappa^{-2}\left(1 - \sqrt{C_f}/\kappa\right) \tag{7}$$

For the non-linear case $\alpha_\tau = \alpha_{\tau\infty}$ is calculated based on Eq. (7) mulitiplied by the ratio $\alpha_{\tau\infty}/\alpha_{\tau 0} = f(\beta)$ given in Figure 2b as determined by Blanckaert and de Vriend (2003).

2.2 *Extension of bed shear stress parametrisations to cover the full width of the channel*

The above bed shear stress parameterizations were developed based on hypotheses that only hold on the centerline. A function is therefore required that extends these parameterisations over the width of the channel.

Many quasi-3D models (e.g. Koch and Flokstra, 1980; Jin and Steffler, 1993) extend Eq. (6) simply by replacing the values for the flow depth and the radius of curvature on the centerline, H and R, resp., by there local values, h(n) and R + n, resp., resulting in the following distribution over the width:

$$f_w(n) = \frac{1}{1+n/R}\frac{h(s,n)}{H} \tag{8}$$

These ad-hoc extensions do not represent correctly the influence of 3D effects on the direction of the bed shear stress. In channels with vertical banks, for example, they would falsely predict a transverse bed shear stress component that violates the boundary condition of zero transverse bed shear stress. Besides the boundary condition of zero value at the banks, the width-distribution was found to be maximum on the centerline and to decrease gradually towards the banks in the experiments reported by Blanckaert (2009, 2010). Therefore, the following width-distribution will be adopted:

$$f_w(n) = \frac{1}{1+n/R}\frac{h(s,n)}{H}\left[1-\left(\frac{2n}{B}\right)^2\right] \tag{9}$$

Eq. (9) extends the description of the angle of the bed shear stress the centerline value given by Eq. (6) over the width of the channel. The effect of this correction to the commonly-used width distribution function (Equation (9)) will be shown further on. The distribution of the increase of bed shear stress ψ is assumed to be constant over the width of the channel.

2.3 *Inertial adaptation*

The parameterization until now neglected inertia. To include effects of inertia the following adaptation equation is used (cf. Jagers 2003).

$$\frac{1}{1+n/R}\frac{\partial hU_sY}{\partial s}+\frac{\partial hU_nY}{\partial n}+\frac{hU_nY}{(1+n/R)R}=\frac{hU}{\lambda}(Y_e-Y) \tag{10}$$

where Y denotes a closure term, α_τ or ψ, and the subscript e should be replaced by 0 for the linear model and ∞ for the non-linear model. The adaptation length λ is chosen according to Johannesson and Parker (1989).

3 MODEL SETUP

3.1 *The experiments*

Two experiments in the sharply curved laboratory flume, shown in Figure 3, were performed by Blanckaert (2009, 2010). The flume has a 9 m long straight inflow reach followed by a 193° bend with a constant centreline radius of curvature of $R = 1.7$ m and a 5 m long straight outflow reach. The width is $B = 1.3$ m and the vertical banks are made of Plexi glas. The bed was composed of nearly uniform sand with diameters in the range $1.6\,\text{mm} < D < 2.2\,\text{mm}$. In the first experiment, a horizontal bed configuration was fixed by spraying paint on it, thus preserving the grain roughness. The second experiment concerned flow over a developed bed topography, but with similar hydraulic conditions. Starting from the horizontal (unfixed) bed, a constant water discharge and constant sediment discharge of ~0.023 kg/(ms) were fed into the flume, while keeping the tailwater depth constant. After the bed level had reached a quasi-equilibrium the bed level was fixed by spraying paint on it in order to allow for detailed velocity measurements.

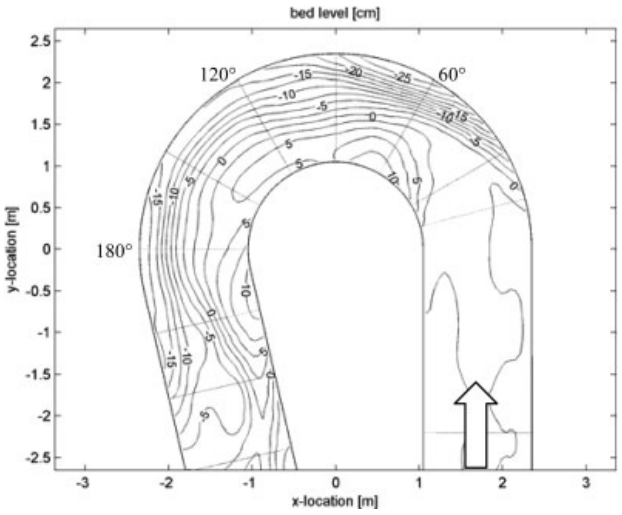

Figure 3. Laboratory flume and developed bed topography referred to average bed level. Flow is from the right to the left.

A pronounced point bar at the inner bend and pool at the outer bend are characteristic features of the resulting equilibrium bed topography, shown in Figure 3. The transversal bed slope increases from ~0° at the bend entry to a maximum value of ~20° in the cross-section situated at 70° into the bend and subsequently shows an oscillating behavior (Fig. 4a). The width averaged bed level shows a uniform streamwise bed slope upstream of the bend. After the bend entrance the width averaged bed level decreases and also shows an oscillating behavior with minima at 90° and about 1.5 meters after the bend. The hydraulic conditions are tabulated in Table 1. H and $U = Q/(BH)$ are the overall mean water depth and velocity. The friction factor has been estimated from the elevation of the water surface above the averaged bed level measured at the centerline, as $1/\sqrt{C_f} = U/(gR_hS_s)^{1/2}$, where R_h is the overall mean hydraulic radius. The values of R/B and R/H indicate a very sharp curvature. Such a sharp curvature constitutes a severe test case for the numerical simulations.

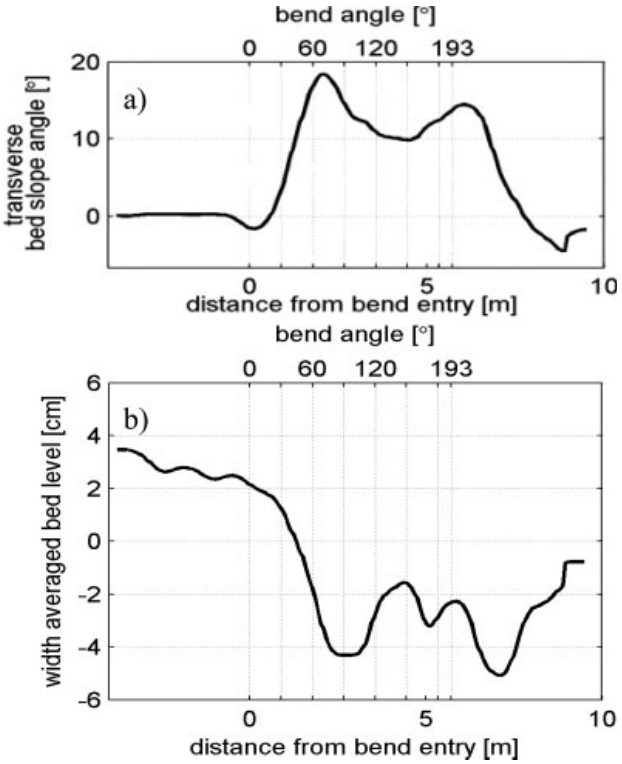

Figure 4. a) Transverse bed slope angle (top) and b) width averaged bed level (bottom) along the bend.

Table 1. Hydraulic conditions.

Case	Q [m^3/s]	H [m]	B [m]	R [m]	R_h [m]	U [m/s]
Horizontal bed	0.089	0.159	1.3	1.7	0.13	0.43
Developed bed	0.089	0.141	1.3	1.7	0.12	0.49
	$C_f^{-1/2}$ [-]	B/R [-]	H/R [-]	R/B [-]	R/H [-]	
Horizontal bed	13.2	0.75	0.094	1.3	10.7	
Developed bed	8.9	0.75	0.083	1.3	12.0	

3.2 *Numerical simulations*

To investigate the applicability of a quasi-3D model in strongly curved bend flow a number of numerical simulations were setup. Two sets of simulations were performed: one set consisted of the flow over a horizontal bed in the flume depicted in Figure 3 and the other set modeled the flow over a fully developed bed situation (also depicted in Figure 3). The study was performed using a research version of the Delft3D (2011) code in 6 modes, which are summarized in Table 2.

The simulations over the horizontal bed parameterized the bed roughness by prescribing a Nikuradse value k_s as three times the median grain diameter (cf. van Rijn 1982). Upstream a discharge of 89 l/s was prescribed and downstream the water level prescribed was 15 cm. The numerical grid consisted of 23 grid points in transverse direction and 156 grid points in streamwise direction. For the three dimensional simulations 4 and 20 layers were used in a sigma coordinate system (cf. Stelling and van Kester, 1994). The simulations over the developed bed used similar characteristics to the horizontal bed experiment, only the downstream water level was set to 11.8 cm. All simulations were run for ten minutes of real time which was sufficient to reach a steady state solution.

Table 2. Models used for the comparison.

Code	Depth averaged	Bed shear stress model	Width Distribution
2DH	Y	N	–
Q3D-L(no width dist)	Y	Y (linear)	N
Q3D-L	Y	Y (linear)	Y
Q3D-NL	Y	Y (nonlinear)	Y
RANS k-ε (4)	N (3D)	(included by calculation)	
RANS k-ε	N (3D)	(included by calculation)	

4 RESULTS

The simulations will be analyzed on three points, namely the evolution of the transverse gradient of the streamwise velocity, the increase of the bed shear stress and the angle between the bed shear stress and the depth averaged flow direction.

4.1 *Transverse gradient of the streamwise velocity*

The redistrition of the streamwise velocity around the bed, as paramterized by α_s (Equation 4) will first be analyzed. The streamwise velocity largely determines the bed shear stress magnitude (Equation 3) and it is the key component of the feedback mechanism in the nonlinear model. The results will only briefly be discussed here. The mechanisms that cause this redistribution are the interplay between secondary flow, topographic steering and curvature variations (cf. Blanckaert & de Vriend 2010 and Ottevanger et al. 2011).

Figure 5a) shows the results of α_s/R over the horizontal bed. In the straight inflow $\alpha_s/R = 0$.At the bend entrance the sudden change in curvature induces an acceleration/deceleration in the inner/outer bend which can be associated to a potential vortex distribution $\alpha_s/R = -1/R$. All models capture this effect reasonably. As the flow moves through the bend secondary flow comes into existence. It can be seen that the 2DH model shows hardly any transverse transport of streamwise momentum through the bend. Q3D-L overestimates the outwards transport of streamwise momentum. Q3D-NL slightly underestimates the outwards transport of streamwise momentum however shows good agreement with the RANS k-ε model. The influence of the secondary flow is reduced due to nonlinear interaction in the case of the Q3D-NL model as a function of the bend parameter β (see curve 1 in Figure 2b). The RANS k-ε model with only 4 layers underestimates the outwards transport of streamwise

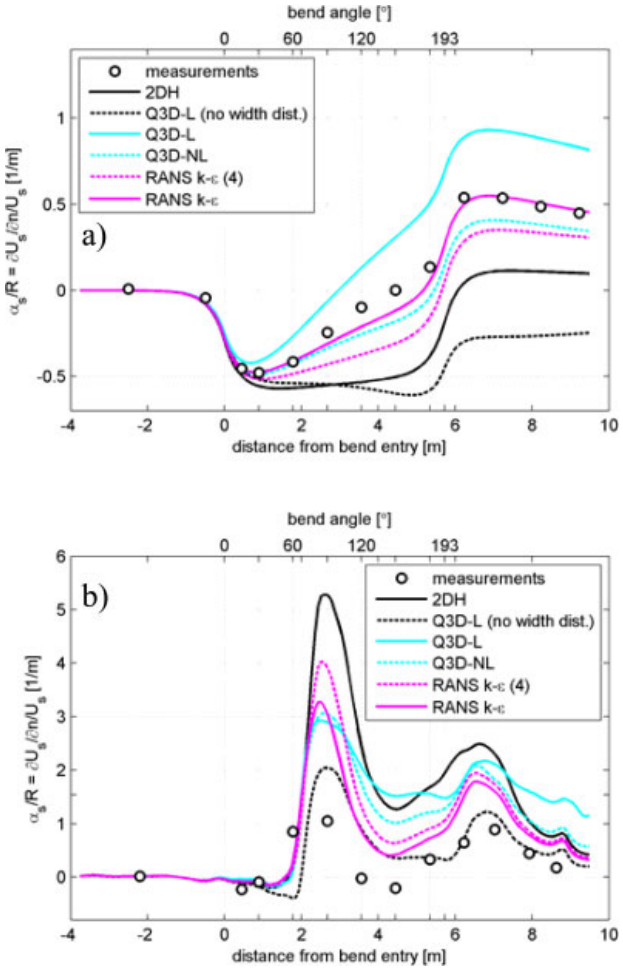

Figure 5. Streamwise evolution of the normalized transverse gradient of the streamwise velocity α_s/R for a) the horizontal bathymetry (top) and for b) the developed bathmetry (bottom).

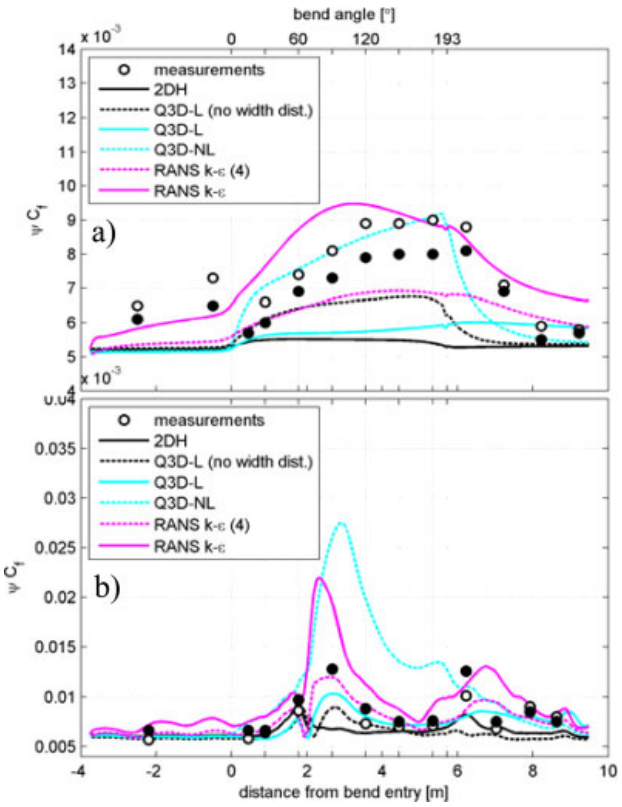

Figure 6. Evolution of the increase of width averaged bed shear stress calculated as $\psi C_f = (\int \tau_b dn/B)/(\int U dn/B)^2$ for the a) horizontal bed case (top) and b) the developed bed case (bottom). The bed shear stress values τ_b from measurements were approximated by fitting a logarithmic profile using $k_s = 6$ mm between 1–2 cm (white dots) and 2–3 cm (black dots) respectively.

momentum more than the Q3D-NL model. The Q3D-L without a width distribution even shows an inward transport of streamwise momentum, which is caused by the unphysical distribution of the secondary flow.

The evolution of α_s/R along the flume over the developed topography is shown in Figure 5b). Qualitatively all curves show approximately the same pattern. This can be explained by the mechanism of topographic steering (Nelson, 1988; Blanckaert, 2010). It may be seen that the pattern in Figure 5b) shows resemblance to the transverse bed level shown in Figure 4a). Quantitively, the RANS k-ε shows the best agreement, while the 2DH strongly overestimates the outward transport of momentum at the 90° section. The Q3D-NL and the RANS k-ε (4) show reasonable agreement with the RANS k-ε, whereas the Q3D-L does not. In the Q3D-NL case secondary flow is almost absent at 150° section in the bend, however the Q3D-L does have secondary flow at this point. This causes the outward transport of streamwise momentum in the Q3D-L case but not in the Q3D-NL case. The latter fits better with the observations. The Q3D-L without a width distribution function also shows good agreement with the measurements. It however has an unphysical distribution of bed shear stresses and secondary flow near the side walls.

4.2 *Increase of bed shear stress*

Using the simulated and measured data we will now compare the modeling of the bed shear stresses for the different models by analyzing ψC_f. Figure 6a) shows the evolution of the width averaged bed shear stress normalized by the width averaged velocity magnitude squared. The results show that in the straight inflow section there is no increase of ψC_f. Through the bend entrance ψC_f increases and finally in the straight outflow section ψC_f decreases again. Only the RANS k-ε and the Q3D-NL model are able to model this increase. The RANS k-ε (4) model underestimates the increase. Upstream of the bend the measured values show some scatter, but it should be realized that it is quite cumbersome to obtain the correct bed shear stresses from ADVP measured velocity profiles close to the bed, due to the uncertainty in the measurements.

Over the developed bed ψC_f is shown in Figure 6b). In this case the measured data show an increase of the ψC_f at the 90° section and at 0.5 m after the bend exit. It is likely that the local increase of ψC_f is partly responsible for the increased depth at the 90° and 1.5 m after the bend (cf Figure 4b). The RANS k-ε model seems to capture this behavior well. The other

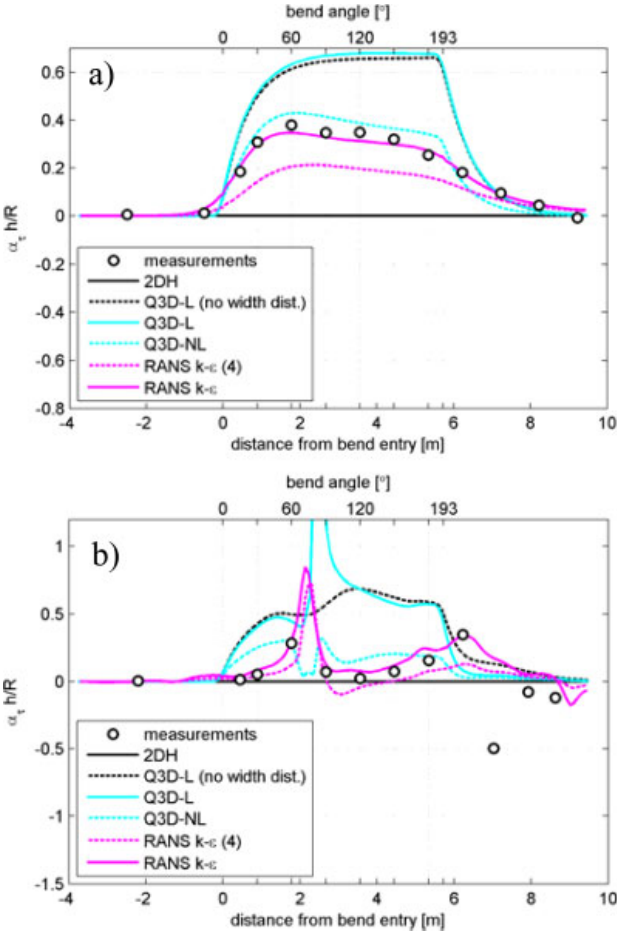

Figure 7. Evolution of the angle between the bed shear stress and the depth averaged flow direction at the centerline (cf. Eq (6)) over a) the horizontal bed (top) and b) over the developed bed (bottom). The direction of the bed shear stress from measurements was approximated by the flow direction in the first 2 cm above the bed.

models, with exception of the Q3D-NL underestimate this effect. The Q3D-NL overestimates ψC_f at the 90° section and does not show the increase of ψC_f after the bend exit as $R = \infty$, cf. Figure 2a).

4.3 *Angle between mean flow direction and bed shear stress direction*

The tangent of the angle between the mean flow direction and the bed shear stress over the horizontal bed is given in Figure 7a). A value of $\alpha_\tau H/R$ equal to one corresponds to an angle between the bed shear and the depth averaged flow direction of 45° directed to the left bank. In the straight inflow section both the bed shear stress and the depth averaged velocity are in the same direction. After the bend entrance it may be observed that the angle between the two increases to a maximum at around 60°–90° and it subsequently decreases. This is related to the secondary flow strength. Beyond the bend there is still a remnant secondary flow cell which slowly decays and induces a difference between the bed shear stress direction and the depth averaged velocity direction.

The 2DH model has no secondary flow model and therefore $\alpha_\tau H/R = 0$. The Q3D-L models overestimate the secondary flow strength through the bend and therefore also overestimate $\alpha_\tau H/R$. Both the RANS k-ε and the Q3D-NL show good agreement with the values obtained from measurements. The RANS k-ε (4) underestimates $\alpha_\tau H/R$.

Over the developed bed the pattern of $\alpha_\tau H/R$ is given in Figure 7b). In the straight inflow section $\alpha_\tau H/R = 0$. After the bend entrance a slight increase $\alpha_\tau H/R$is observed. Towards the 120° section$\alpha_\tau H/R$ decays to almost zero. Towards the end of the bend an increase in $\alpha_\tau H/R$occurs. After the bend exit $\alpha_\tau H/R$ increases even further. Subsequently at about 2 meters downstream of the bend exit a strong negative value is found (direction of the bed shear stress is less directed to the inner bank than the depth averaged flow), which is possibly related to an erroneous experimental value. Subsequently the angle tends to the straight channel limit. The 2DH model implies by definition $\alpha_\tau H/R = 0$. The Q3D-L models overestimate the angle between the bed shear stress and thesecondary flow. The Q3D-NL model slightly overestimates the angle at the bend entrance. It subsequently underestimates the peak after the bend exit. The RANS k-ε as well as the RANS k-ε (4) show a similar oscillating behavior. Both models exhibit a strong peak near 75° which coincides with the peak zone of outward streamwise momentum redistribution (cf Figure 5b). This is not yet fully understood.

The angle of the bed shear stress vector is considered to be an essential component of the morphological development of the point bar. Based on the results in Figure 7 and Eq. (5), it is likely that, if coupled to a sediment transport model, the 2DH would underestimate the point bar height, the Q3D-L models would overestimate the point bar height and the RANS and Q3D-NL models would provide the closest results to the double point bar (cf. Figure 4a).

Table 3. Simulation times for the different numerical simulations.

Case	Horizontal bed	Developed bed
2DH	35″	1′05″
Q3D-L(no width dist)	55″	2′27″
Q3D-L	1′16″	2′24″
Q3D-NL	1′29″	2′48″
RANS k-ε (4)	2′41″	5′00″
RANS k-ε	22′07″	41′32″

4.4 *Simulation times*

Besides the comparison of the results, the simulation times were also analyzed (see Table 3). The Q3D simulations typically took 2 to 2.5 times longer than the depth averaged model. Compared to the detailed RANS simulations the Q3D simulations were around 13 times faster for the horizontal topography and around 8 times faster over the developed topography. Compared to the coarse RANS model the Q3D model was approximately twice as fast.

5 CONCLUSIONS

In the present investigation the focus was on the quasi-3D modeling of bed shear stresses for strongly curved bends. Using measurement data, RANS models, a 2DH model and Q3D models valid for mildly curved and strongly curved flows an analysis of the bed shear stresses was done on two points: firstly the increase of friction due to curvature and secondly the angle between the bed shear stress and the depth averaged flow direction on the centreline.

The increase of friction was well captured by the Q3D-NL model and the RANS k-ε model over the horizontal bed. Over the developed bed the RANS k-ε model showed good agreement with the measured data. The Q3D-NL model overestimated the increase halfway through the bend and failed to reproduce the increase after the bend exit. The 2DH and Q3D-L models did not succeed in modeling the increase of friction through the bend as it is not included in the models. The coarse RANS k-ε model under predicted the increase of friction in both cases.

The tangent of the angle between the depth averaged flow and the bed shear stress was well modeled by the Q3D-NL and RANS k-ε model over the horizontal bed. The coarse RANS k-ε underestimated the angle of the bed shear stress, due to a lack of resolution in the boundary layer. Over the developed bed the magnitude was well approximated by the Q3D-NL and RANS k-ε models. The Q3D-NL model and the RANS models showed an oscillating behavior through the bend. The Q3D-L models overestimated the angle, whereas the 2DH angle was always zero for both the horizontal and the developed bed. Over the developed bed the Q3D-L models did not show an oscillating behavior.

We have shown that quasi-3D models give a reasonable prediction of the processes caused by the three dimensionality of the flow in sharp open channel bends and they are indeed faster than their three dimensional counterparts.

ACKNOWLEDGEMENTS

The Dutch Technology Foundation (STW, applied science division of NWO) is acknowledged for funding the PhD research of the first author under grant DCB.7780. The support of Deltares is also gratefully acknowledged. Finally, Hanneke Nijhof is thanked for help with the figures. Blanckaert was partially funded by the Chinese Academy of Sciences Visiting Professorship for Senior International Scientists, grant number 2011T2Z24, by the Sino-Swiss Science and Technology Cooperation for the Institutional Partnership Project, grant number IP13_092911.

REFERENCES

Blanckaert, K. (2009), Saturation of curvature-induced secondary flow, energy losses, and turbulence in sharp open-channel bends: Laboratory experiments, analysis, and modeling, J. Geophys. Res., 114, F03015

Blanckaert, K. (2010), Topographic steering, flow recirculation, velocity redistribution, and bed topography in sharp meander bends, Water Resour. Res., 46, W09506

Blanckaert, K. and de Vriend, H. J. (2003). "Non-linear modeling of mean flow redistribution in curved open channels." Water Resour. Res. 39(12), 1375.

Blanckaert, K., and H. J. de Vriend (2010), Meander dynamics: A nonlinear model without curvature restrictions for flow in open – channel bends, J. Geophys. Res., 115, F04011.

Camporeale, C., P. Perona, A. Porporato, and L. Ridolfi (2007), Hierarchy of models for meandering rivers and related morphodynamic processes, Rev. Geophys., 45

De Vriend H. J. (1977). "A mathematical model of steady flow in curved shallow channels." J. Hyd. Res., 15(1), 37–54,

Delft3D (2011) User Manual. http://oss.delft3d.nl

Engelund, F. (1974), Flow and bed topography in channel bends, J. Hydraul. Div. A.S.C.E., 100(HY11), 1631–1648.

Jagers, H. R. A. (2003) "Modelling planform changes of braided rivers". Phd thesis. University of Twente.

Jin Y.-C. and Steffler P. M. (1993). "Predicting flow in curved open channels by depth-averaged method." J. Hydr. Engng, ASCE, 119(1), 109–124.

Johannesson H. and Parker G. (1989), Secondary flow in a mildly sinuous channel, J. Hydraul. Eng., 115(3), 289–308,

Johannesson H. and Parker G. (1989b). "Velocity redistribution in meandering rivers." J. Hydr. Engng, ASCE, 115(8), 1019–1039.

Kikkawa, H., S. Ikeda, and A. Kitagawa (1976), Flow and bed topography in curved open channels, J. Hydraul. Div. Am. Soc. Civ. Eng., 102(HY9), 1327–1342.

Koch, F.G. and C. Flokstra, 'Bed level computations for curved alluvial channels,' Proc. XIX Congress of the IAHR, Vol. 2, New Delhi, India, p. 357, 1980.

Mosselman, E. (2005) Basic Equations for Sediment Transport in CFD for Fluvial Morphodynamics, in Computational Fluid Dynamics: Applications in Environmental Hydraulics (eds P. D. Bates, S. N. Lane and R. I. Ferguson), John Wiley & Sons, Ltd, Chichester, UK.

Nelson, J.M., (1988). Mechanics of Flow mad Sediment Transport over Nonuniform Erodible Beds. Ph.D. Dissertation, Univ. of Washington, Seattle, Wash.

Olesen K. W. (1987). "Bed topography in shallow river bends." Report No. 87-1, Dept. Civ. Eng., Delft Univ. Techn., Delft.

Ottevanger, W., Blanckaert K., Uijttewaal W.S.J. (2011). Processes governing the flow redistribution in sharp river bends. Geomorphology

Stelling, G.S. and van Kester J.A.Th.M. (1994). On the approximation of horizontal gradients in sigma coordinates for bathymetry with steep bottom slopes. Int. J. Num. Meth. Fluids, Vol. 18, 915–955.

Rozovskii, I. L. (1957). Flow of Water in Bends of Open Channels. Isr. Progr. Sc. Transl., Jerusalem, 1961.

Vardy, A. (1990). Fluid principles. England: McGraw-Hill

Van Rijn, L. C. (1982). "Equivalent Roughness of Alluvial Bed". J. of the Hydr. Div., ASCE, Vol. 108, No. HY10